Separation Science and Technology
Publication details, including instructions for authors and subscription information:
http://www.informaworld.com/smpp/title~content=t713708471

Recovery and Concentration of Metal Ions. IV. Uphill Transport of Zn(II) in a Multimembrane Hybrid System

Romuald Wódzki[a]; Grzegorz Sionkowski[a]; Gryzelda Poźniak[b]
[a] FACULTY OF CHEMISTRY, NICOLAUS COPERNICUS UNIVERSITY, TORUŃ, POLAND [b] INSTITUTE OF ORGANIC AND POLYMER TECHNOLOGY, TECHNICAL UNIVERSITY OF WROCŁAW, WROCŁAW, POLAND

Online publication date: 03 August 1999

To cite this Article Wódzki, Romuald , Sionkowski, Grzegorz and Poźniak, Gryzelda(1999) 'Recovery and Concentration of Metal Ions. IV. Uphill Transport of Zn(II) in a Multimembrane Hybrid System', Separation Science and Technology, 34: 4, 627 — 649
To link to this Article: DOI: 10.1081/SS-100100671
URL: http://dx.doi.org/10.1081/SS-100100671

SEPARATION SCIENCE AND TECHNOLOGY, **34**(4), pp. 627–649, 1999

Recovery and Concentration of Metal Ions. IV. Uphill Transport of Zn(II) in a Multimembrane Hybrid System

ROMUALD WÓDZKI* and GRZEGORZ SIONKOWSKI
FACULTY OF CHEMISTRY
NICOLAUS COPERNICUS UNIVERSITY
87-100 TORUŃ, POLAND

GRYZELDA POŹNIAK
INSTITUTE OF ORGANIC AND POLYMER TECHNOLOGY
TECHNICAL UNIVERSITY OF WROCŁAW
50-370 WROCŁAW, POLAND

ABSTRACT

A study has been made on the uphill transport of zinc cations across a multimembrane hybrid system (MHS) composed of two ion-exchange membranes (IEM) separated by a bulk liquid membrane (BLM). The fluxes of the Zn(II)/H countertransport were investigated as dependent on the composition and structure of ion-exchange polymer membranes (i), the solvent of a liquid membrane (ii), the feed and strip membrane area ratio (iii), and the pH of the feed solution (iv). The IEMs of various ionogenic groups (sulfonic acid, carboxylic acid, quaternized amine) and of various structure (clustered, gelatinous, porous) were examined in the MHS containing the BLM with di(2-ethylhexyl)phosphoric acid as a carrier of Zn(II) cations. It has been found that the Zn(II) fluxes are dependent on the properties of both the BLM and polymer membranes, i.e., on the BLM solvent viscosity (i), the nature and concentration of the IEM ion-exchange sites (ii), and the IEM thickness (iii). The best results were obtained when using hexane as the BLM solvent and the Nafion-117 membrane (perfluorinated polymer, sulfonic acid groups) as the cation-exchange membrane (CEM). The influence of the area ratio (feed-to-strip interface) has been checked for A_f/A_g equal to 3:1, 1:1, and 1:3. It was found that the asymmetry of the system leads mainly to some changes in the accumulation of transported species in a liquid membrane phase.

*To whom correspondence should be addressed.

INTRODUCTION

The simplest multimembrane hybrid system (MHS) for ionic species transport is composed of a bulk liquid membrane (BLM) placed between two solid ion-exchange polymer membranes (IEM) contacted with the aqueous feed and strip solution. The cation transfer mechanism (see Fig. 1) results from two different processes, i.e., the diffusion coupled with ion-exchange reactions in a cation-exchange membrane (CEMs), and the countertransport of cations me-

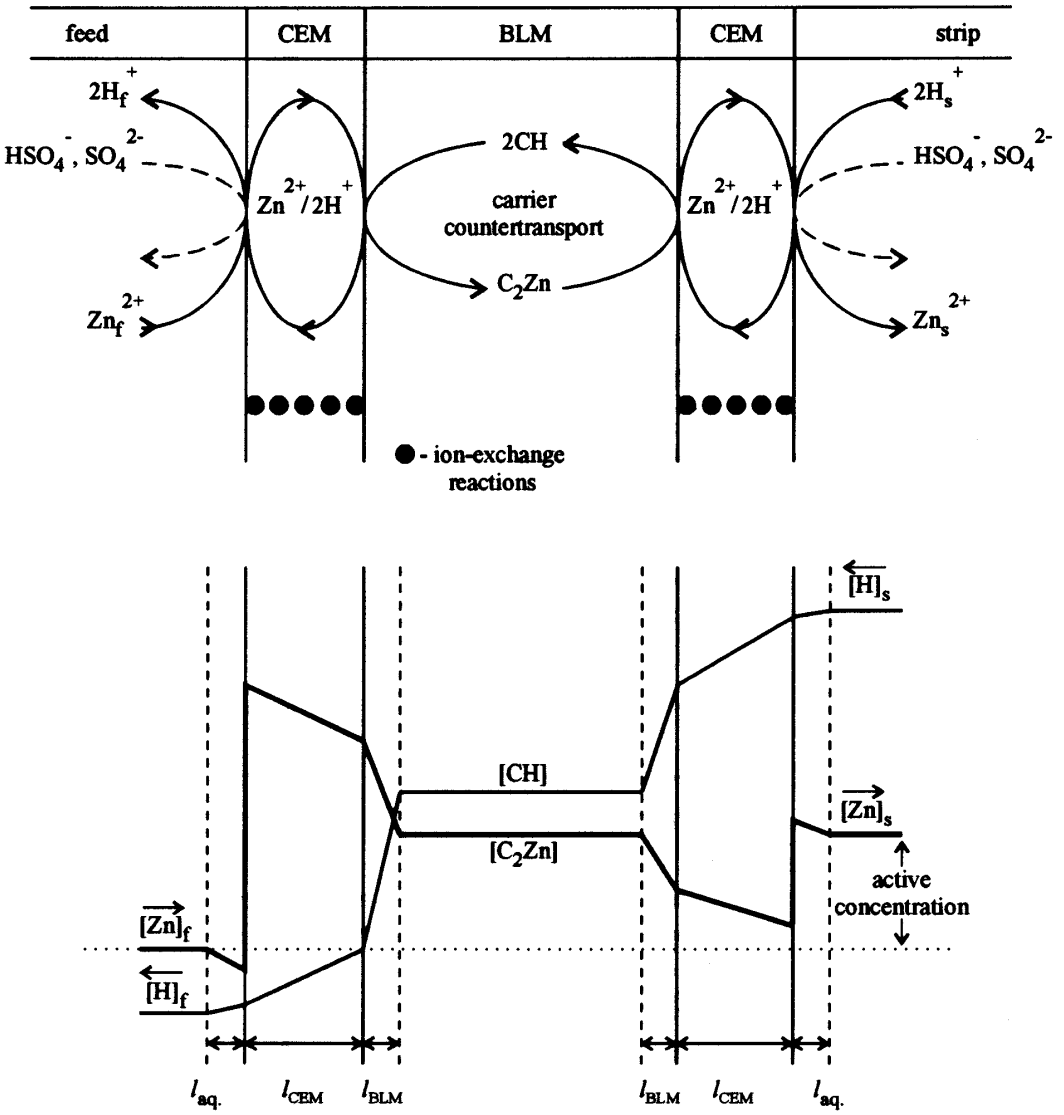

FIG. 1 Schematic representation of MHS transport mechanism and possible concentration profiles of transported species. CEM = cation exchange membrane, BLM = agitated bulk liquid membrane.

MARCEL DEKKER, INC.
270 Madison Avenue, New York, New York 10016

diated by the carrier in the BLM. Both processes involve several reaction–diffusion steps presented in Fig. 1 with possible concentration profiles for all species permeating the MHS [when used for the Zn(II) enrichment in the stripping solution].

It was demonstrated elsewhere that an MHS composed of physically different membranes can be used for the recovery and separation of metal ions (1, 2) or some carboxylic acids (3). In this paper we report on the active concentration of Zn(II) and its dependence on operating conditions and the MHS composition. Among various metal ions, Zn(II) appears in many waste streams from hydrometallurgy and surface-treatment industries. Wastewater polluted by zinc can be purified by using liquid membranes to the level of 0.5 mg Zn/dm^3 ($8 \times 10-6$ mol/dm^3). A typical example (4) is the reduction of Zn(II) concentration from 0.05 mol/dm^3 to some ppm with a simultaneous enrichment of the stripping solution up to 0.76 mol Zn/dm^3. This requires efficient transport of Zn(II) from a diluted to concentrated solution, also called "uphill" transport or chemical pumping. In general, the coupled transport of charged species against their concentration difference is mediated by a carrier and driven by simultaneous downhill transport of another charged solutes present excessively in the receiving solution. Some other reaction processes (e.g., complexation, association, redox) occurring in the receiving bulk solution and acting as an additional driving force can amplify the overall effect of active concentration.

The aim of this work has been to check MHS performance during the concentration of Zn(II) ions in the following system:

$$\text{(feed) } ZnSO_4 \text{ aq soln}|\text{MHS}|ZnSO_4 + H_2SO_4 \text{ aq soln (strip)}$$

The aqueous solution initially containing metal ions transported by the MHS is referred to as the feed solution (f). The solution of the same metal concentration, but with added sulfuric acid, is present at the opposite side of the MHS and used as the strip (or receiving) solution (s). According to the scheme in Fig. 1, hydrogen ions (pumping ions) balance and drive the flow of Zn(II) ions. One can expect that transport phenomena in the system are dependent on the properties of both the IEMs and the BLM used to construct the MHS. The following features of any IEM may be important for the MHS operation: the kind and density of ionogenic groups (i), the membrane swelling and thickness (ii), the chemical composition of the membrane backbone (iii), and the membrane permselectivity (5) necessary to protect the system against sorption and diffusion of free electrolytes (iv). Regarding the properties of a liquid membrane, the properties of the carrier and solvent can control the MHS operation. Specifically important for the MHS are properties such as the ability of a carrier to transport Zn(II) ions in the wide range of feed pH (v), and low liquid membrane viscosity and miscibility with water (vi).

Moreover, the properties of the MHS and external solutions should be taken into account to explain basic conditions for the uphill transport. In the simplest case of the univalent cations (M and H) countertransport, the stationary flux under diffusion limited conditions is (6, 7)

$$J_{\mathrm{M}} = J_{\max} \times \frac{[\mathrm{M}]_{\mathrm{f}}[\mathrm{H}]_{\mathrm{s}} - [\mathrm{M}]_{\mathrm{s}}[\mathrm{H}]_{\mathrm{f}}}{([\mathrm{H}]_{\mathrm{f}} + K_{\mathrm{H}}^{\mathrm{M}}[\mathrm{M}]_{\mathrm{f}})([\mathrm{H}]_{\mathrm{s}} + K_{\mathrm{H}}^{\mathrm{M}}[\mathrm{M}]_{\mathrm{s}})} \tag{1}$$

where

$$J_{\max} = \frac{D[\mathrm{C}]K_{\mathrm{H}}^{\mathrm{M}}}{2l_{\mathrm{BLM}}} \tag{2}$$

In Eqs. (1) and (2), l_{BLM} denotes the thickness of diffusion layers in the BLM, D is the diffusion coefficient of a carrier, and [C] is its concentration. The constant $K_{\mathrm{H}}^{\mathrm{M}}$ is the equilibrium constant for the simplest ion-exchange reaction:

$$\mathrm{M}^{+} + \mathrm{CH} \leftrightarrow \mathrm{CM} + \mathrm{H}^{+} \tag{3}$$

Equations (1) and (2) describe a bulk liquid membrane contacted immediately with aqueous solutions. These equations can also be applied in the case of the BLM operating in the MHS, but the respective feed and strip concentrations should be interpreted as related to the feed and strip CEM.

It is evident from Eq. (1) that the flux of M^{+} cations in the coupled transport is always positive when

$$[\mathrm{M}]_{\mathrm{f}}[\mathrm{H}]_{\mathrm{s}} > [\mathrm{M}]_{\mathrm{s}}[\mathrm{H}]_{\mathrm{f}} \tag{4}$$

This is the main difference in respect to the usual diffusion where the flux is positive only for $[\mathrm{M}]_{\mathrm{f}} > [\mathrm{M}]_{\mathrm{s}}$. Note that the term "uphill" transport (or secondary active transport) concerns the external concentrations [M] and [H], and does not mean the permeation of a carrier inside the LM against its own concentration gradient. In other words, the transport remains passive when considering the properties of the liquid membrane alone. The flux equation for a system with a divalent–univalent cation-exchange reaction is more complex (8):

$$J_{\mathrm{M}} = J_{\max}\left(R_{\mathrm{f}} - R_{\mathrm{s}} + \sqrt{R_{\mathrm{s}} + R_{\mathrm{s}}^2} - \sqrt{R_{\mathrm{f}} + R_{\mathrm{f}}^2}\right) \tag{5}$$

where

$$R_i = \frac{[\mathrm{H}]_i^2}{8[\mathrm{C}]K_{\mathrm{H}}^{\mathrm{M}}[\mathrm{M}]_i}, \qquad \text{for } i \equiv \mathrm{f} \text{ or } \mathrm{s} \tag{6}$$

The underlying ion-exchange reactions and the overall equilibrium condition

MARCEL DEKKER, INC.
270 Madison Avenue, New York, New York 10016

for the system allow one to conclude that the transport will occur when the following nonequality is fulfilled:

$$[M]_f[H]_s^2 > [M]_s[H]_f^2 \tag{7}$$

The uphill transport phenomena in ion-exchange polymer membranes were discussed several years ago by Lakshminarayanaiah (9) as typical diffusion processes in multi-ionic membrane systems. This process can also be interpreted as the transport mediated by a fixed carrier (10) or, in a more simple way, as the Donnan dialysis (ion-exchange dialysis) occurring in the system:

$$\text{(f) } M^{n+}|\text{cation-exchange membrane}|H^+ \text{ (s)}$$

The driving force (DF) for this process (11) is

$$DF = RT \ln \left(\frac{[M]_f^n[H]_s}{[M]_s^n[H]_s} \right)^{1/n} \tag{8}$$

and the uphill transport conditions are similar to these described by Eq. (7). However, it is difficult to formulate one compact transport equation for the MHS, because all the ionic fluxes are coupled to interfacial reactions occurring simultaneously. This can be accomplished by using network thermodynamic analysis (12, 13) as a technique suitable for describing reaction–diffusion phenomena.

Equations (1)–(8) prove that MHS uphill transport may be achieved independently owing to some properties of solid or liquid ion-exchange membranes which enable ion-exchange dialysis and/or coupled carrier transport, respectively. Moreover, according to Eqs. (4) and (7), external solutions must fulfill some specific conditions in order to maintain suitable driving forces. Additionally, it should be explained that the theoretical equations concern species actually transported, i.e., cations exchanged by the components of the BLM and the CEMs. Thus, the term “secondary active transport” deals with proper changes of concentrations of the same ions in the external reservoirs. In practice, however, the experimental uphill transports also involve some additional stripping processes dependent on the composition of a receiving solution. Usually these processes exclude some ions from transport phenomena by complexation or formation of other un-ionized but soluble compounds. In the system based on Zn(II)/H exchange between the feed and strip solution containing sulfuric acid, the sulfate anions can act as a stripping agent which promotes the formation of some associates or complexes of various compositions (23). This means that from a theoretical point of view the transport can remain downhill despite experimentally observed uphill transport effects leading to $[Zn]_s > [Zn]_f$. Consequently, the results presented in this paper, as re-

lated to the overall zinc content in the feed and strip solutions, should be considered as effective uphill transport with possible secondary active transport phenomena.

EXPERIMENTAL

Transport System and Cell Construction

The apparatus used for transport experiments was the same as the one described in earlier papers (1, 2) except for the cell construction being substantially changed. The permeation studies were carried out in a cell of "the multiwindow type" designed specially for this study. The details of the cell construction are presented in Fig. 2. The effective surface area of each window was 2.92 cm^2. With two out of four compartments acting as the feed intermediate reservoirs (f), and the other two as receiving compartments (s), the cell provided a symmetric transport system, with a working membrane area of 5.85 cm^2 for the feed and strip interface. In other configurations the cell enabled us to make experiments with the feed-to-strip area ratio equal to 3:1 or 1:3, i.e., with 8.75 cm^2 for the feed and 2.92 cm^2 for the strip interface. Solutions from the external reservoirs [500 (f) and 100 (s) cm^3] were circulated in the system by running a multichannel peristaltic pump (Gilson, Minipuls 3). Volumetric flow rates for feed and strip solutions were 2.5 cm^3/min. The solutions flowed at this rate through contact compartments (1a and 2a in Fig. 2) with volumes of ca. 1 cm^3 each. There was no pressure difference between aqueous solutions and liquid membranes as a result of pumping. As shown in Fig. 2, the external solutions were supplied to "open" contact compartments in a transport cell by exploiting the concept of the transfusing cell, i.e., the upper level of a liquid was maintained by more efficient repumping. At zero time, each of compartments contained zinc sulfate of equal concentration, usually 1×10^{-3} mol/dm^3, as a typical concentration of rinse solutions appearing in electroplating installations. The driving force for the uphill transport of Zn(II) was generated by a higher concentration of sulfuric acid (0.1 mol/dm^3) added to the strip solution. A Teflon-made element with ion-exchange membranes was inserted into a glass vessel containing an agitated (300 rpm, magnetic stirrer, Heidolph MR2000) bulk liquid membrane with a volume of 35 cm^3. The cell and solutions were thermostated at 25 ± 0.5°C by an air thermostat.

The flow of zinc ions across the MHS was followed in time, up to 70 hours, by a calibrated AA spectrophotometer. The samples for analysis (0.5 cm^3) of the feed and strip solutions were taken from the external reservoirs (1 and 2, Fig. 2). The respective concentrations are denoted $[Zn]_f$ and $[Zn]_s$. The pH values of the feed were monitored on-line with a pH meter.

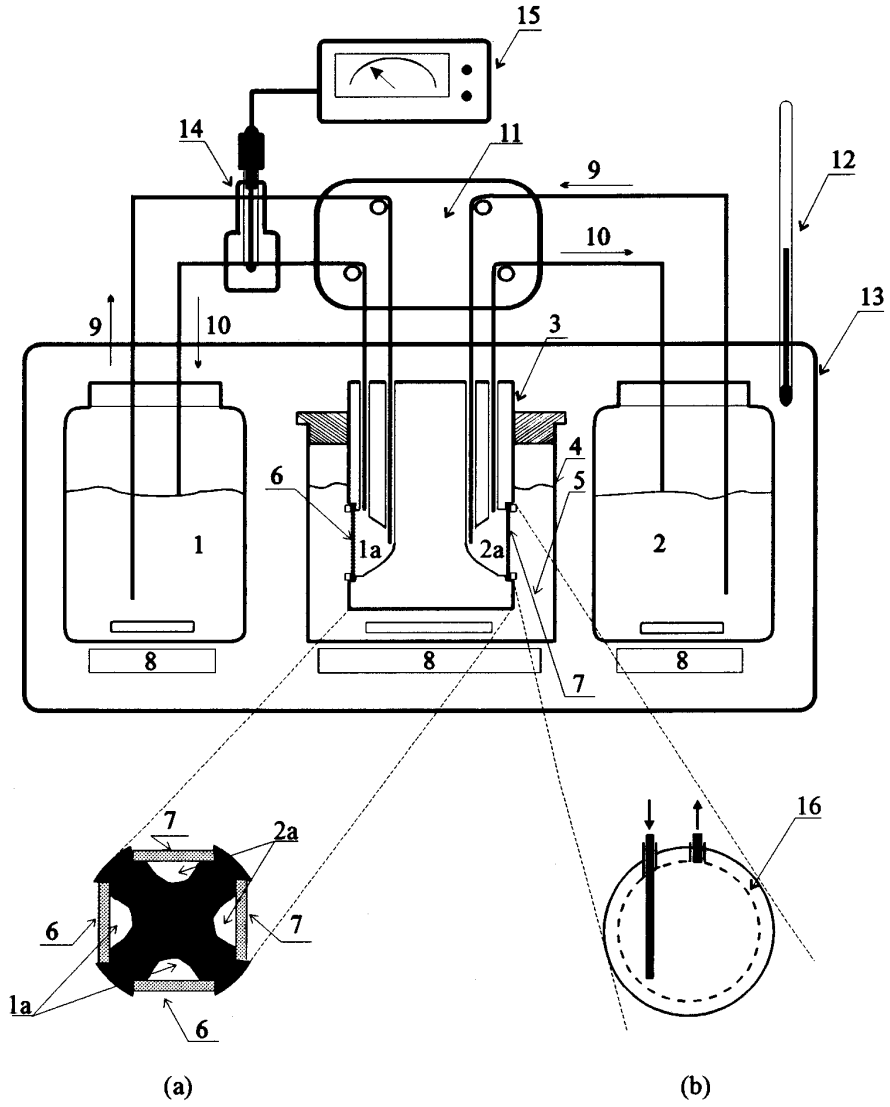

FIG. 2 Scheme of the transport system and cell construction: feed solution (1), strip solution (2), feed (1a) and strip (2a) contact chamber, Teflon-made cell, (3), glass vessel (4), bulk liquid membrane (5), feed cation-exchange membrane (6), strip cation-exchange membrane (7), magnetic stirrer (8), feed and strip inlet (9) and outlet (10), peristaltic pump (11), air thermostat (12, 13), pH electrode (14), pH meter (15), ring (16); horizontal (a) and vertical (b) cross section of contact chamber.

Liquid Membrane

The bulk liquid membrane as a part of the MHS was composed of an organic solvent containing dissolved di(2-ethylhexyl)phosphoric acid (D2EHPA) purchased from SIGMA, USA. The concentration of D2EHPA was always 0.01 mol/dm^3 except as noted below. A fresh solution of the BLM

was used for each of transport runs. The BLM was stirred by magnetic bars as shown in Fig. 2. During introductory experiments a stirring rate was increased until a constant flux was reached. Thus, by carrying out the experiments with the BLM stirred at a rate of 300 rpm, the boundary-layer resistances were diminished as far as possible.

A membrane phase was prepared from such diluents as kerosene (MAKER, Poland, bp 124–174°C, viscosity 0.68 cP), toluene, carbon tetrachloride, and hexane. Kerosene was a technical grade solvent whereas the others were analytical grade reagents.

Ion-Exchange Polymer Membranes

Some commercially available ion-exchange membranes of different compositions were used to arrange the MHS. Their basic properties, including the concentration of ion-exchange sites, swelling in water, and thickness, are listed in Table 1. The ion-exchange capacity and water content were determined for each set of membrane samples used in the transport experiments. The ion-exchange capacity (in moles of functional groups per kilogram of sorbed water) of strong-acid cation-exchange membranes was measured by converting the membrane sample to its hydrogen form in 2 M HCl, and then (after washing in distilled water), by exchanging hydrogen ions in 1 M NaCl solution. The resultant solution, containing reexchanged hydrogen ions, was then titrated with 0.1 M NaOH. In the case of the strong-base anion-exchange membrane, the procedure was similar except for changing the reagents, i.e., the membrane previously converted to the OH form was placed in the NaCl solution. Then released hydroxide ions were titrated potentiometrically with acid solution. The Flemion samples in their hydrogen form were neutralized with a measured volume of the 0.1 M NaOH solution titrated further on. The ion-exchange capacity was then calculated from the difference between the initial and the final concentrations of NaOH solution used.

Before transport experiments, the feed and strip IEM membranes were preequilibrated with the feed or the strip solution in order to minimize the possible accumulation of metal ions in the cation-exchange membranes (CEMs) during a transport experiment. The membranes were placed in 25 cm^3 of the feed (1×10^{-3} M $ZnSO_4$) or strip (1×10^{-3} M $ZnSO_4$ + 0.1 M H_2SO_4) solution. The solutions were changed three times (after each 3 hours of equilibration), and then the membranes were left in the fresh solutions for 12 hours. The membranes were wiped with hard filter paper before being placed in the transport cell. The ion-exchange capacity vs Zn(II) (feed samples only) was checked by analyzing the zinc content in the membrane sample after reexchanging in 0.5 M H_2SO_4. It was found that the amount of Zn exchanged by the samples of CEMs was always 95% or higher of the value predicted from the standard ion-exchange capacity presented in Table 1. The water content in

TABLE 1
Ion-Exchange Membrane Characteristics

Membrane and producer	Composition	Concentration of ion-exchange groups[a]	Water content (wt%)		Thickness cm		Ref.
			(f)[b]	(s)[c]	(f)[b]	(s)[c]	
Nafion-120	Sulfonic groups attached to perfluorinated polymer backbone, EW = 1200	4.3 mol —SO_3H/kg H_2O	13.7	12.8	0.030	0.028	24
Nafion-117 Du Pont de Nemours, USA	Sulfonic groups attached to perfluorinated polymer backbone, EW = 1100	3.9 mol —SO_3H/kg H_2O	17.7	19.7	0.022	0.022	24
Raipore 4010 Raipore Corp., USA	Styrene sulfonate grafted onto fluorinated polymer backbone	2.8 mol —SO_3H/kg H_2O	27.3	30.7	0.005	0.005	
MRF-26 Gos.Inst.Prikl.Khim., Russia	α,β,β′-Trifluorostyrenesulfonic acid grafted onto copolymer of fluorovinylidene and hexafluoropropylene	2.8 mol —SO_3H/kg H_2O	19.5	23.3	0.028	0.027	25
Flemion Asahi Glass, Japan	Carboxylic groups attached to perfluorinated polymer backbone	15.7 mol —COOH/kg H_2O	10.3	9.2	0.017	0.017	26
Neosepta CM-1	Sulfonic groups attached to crosslinked polystyrene backbone, reinforced	3.1 mol —SO_3H/kg H_2O	36.1	34.5	0.015	0.015	27
Neosepta CM-2 Tokuyama Soda, Co. Ltd., Japan		4.8 mol —SO_3H/kg H_2O	27.7	27.3	0.013	0.013	27
Neosepta AFN-7 Tokuyama Soda, Co. Ltd, Japan	Quaternary ammonium groups attached to crosslinked polystyrene backbone, reinforced	7.1 mol —$N(CH_3)OH$/kg H_2O	40.2	38.4	0.016	0.016	27
SPS-1, laboratory-made	Sulfonated polysulfone	0.30 mol —SO_3H/kg dry polymer	84.0	83.5	0.015	0.015	14
SPS-2, laboratory-made		0.65 mol —SO_3H/kg dry polymer	84.4	83.4	0.016	0.014	14

[a] Cation-exchange membranes in H^+ form, anion-exchange membrane in OH form.
[b] After equilibration in 1×10^{-3} M $ZnSO_4$.
[c] After equilibration in 1×10^{-3} M $ZnSO_4$ + 0.1 M H_2SO_4.

Marcel Dekker, Inc.
270 Madison Avenue, New York, New York 10016

the feed and strip membrane (Table 1) was determined from the mass of the swollen and dried (110°C) membrane sample.

Synthesis of Sulfonated Polysulfone (SPS) Membranes

The asymmetric SPS membranes (14) were synthesized to obtain new ion-exchange membranes with a reduced thickness of the dense ion-exchange layer. The following materials and procedures were applied in order to synthesize SPS.

Polysulfone (PS)—The polymer was commercially available from Amoco Performance Products (Atlanta, GA, USA) under the trademark Polysulfone P-1700. Its weight-average molecular weight is approximately 75,000 and its number-average weight is approximately 35,000.

Sulfonated polysulfone (SPS)—PS was sulfonated according to a procedure described by Brousse et al. (15) after dissolving it in 1,2-dichloroethane. The reaction was carried out with a 0.5:1 or 0.95:1 acid-to-monomer molar ratio for 1.5 hours at room temperature. Chlorosulfonic groups were then hydrolyzed in a 5 M solution of NaOH in butanol (24 hours, room temperature).

Membrane preparation and properties—The membranes were formed by the phase inversion method after dissolving SPS in *N*,*N*′-dimethylformamide (20 wt% solution). The solution was cast on a glass plate, doctor bladed, and immediately immersed in water. The membranes were stored under water at least 1 week before use. Their degree of sulfonation was calculated from their analytically determined sulfur content. The ion-exchange capacity of the polymer-forming membrane was determined by potentiometric titration with sodium hydroxide of the SPS-H form in a mixture of DMF (90 vol%) and water (10 vol%) (16). The ion-exchange capacity was 0.30 and 0.65 (in mol/kg dry H^+ form) for the membrane with degrees of sulfonation equal to 0.14 (SPS-1) and 0.31 (SPS-2), respectively. The thickness and swelling of the membranes are listed in Table 1. The membranes in their swollen state are highly porous (except for a skin layer), and their overall water content amounts to 84 vol%.

RESULTS AND DISCUSSION

Transport Conditions

Typically for transports in a diaphragm cell, the experimental studies were carried out using a standard "quasi-steady-state" method. The method requires all parameters to be held constant except for the stripping concentration which can vary slowly with time. In the case of a bulk membrane of rather large volume, some additional nonstationary effects can be caused by a time-dependent accumulation of transported species inside the membrane phase. Therefore, the initial and boundary conditions for the studied transports may be impor-

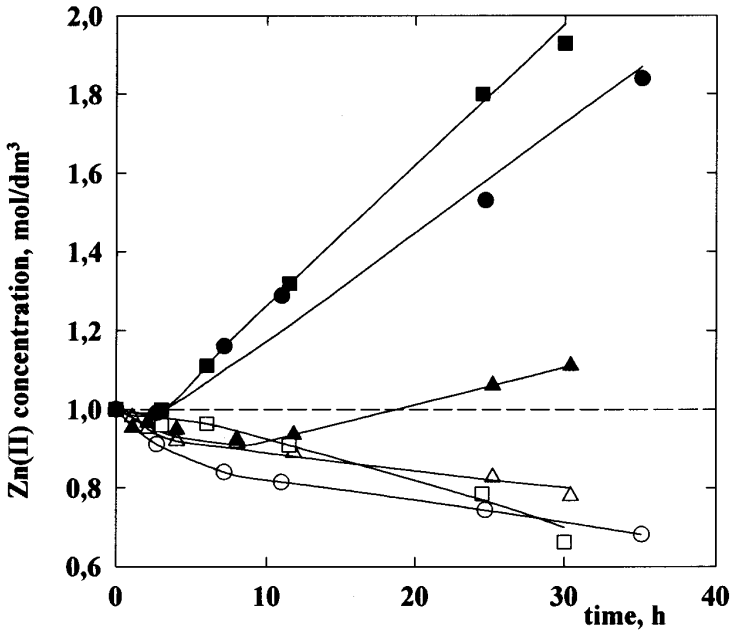

FIG. 3 Feed (empty symbols) and strip (filled symbols) Zn(II) concentration versus time for different zero-time conditions. The systems are (△, ▲) 0.1 M D2EHPA and Nafion-120 membranes in their hydrogen form; (□, ■) 0.1 M D2EHPA and preequilibrated Nafion-120 membranes; and (○, ●) 0.01 M D2EHPA and preequilibrated Nafion-120 membranes.

tant in order to reach a quasi-steady-state regime. For example, the concentration of a carrier in a liquid membrane, as well as the initial ionic form of polymer membranes, can affect the time of a transient state, as seen in Fig. 3. When the feed and strip CEMs are in their starting hydrogen form, the minimum for $[Zn]_s = f(t)$ caused by an overall ion-exchange capacity of the MHS is very large and the negative influx of Zn(II) from the strip into the MHS is noticeable. The minimum diminishes markedly when the membranes are preconditioned in their respective aqueous solutions, and the concentration of D2EHPA in the BLM is reduced to 1×10^{-2} mol/dm^3. From the plots presented it can be concluded that, after the time required to attain quasi-steady-state operation, the concentration data are suitable for calculating steady-state uphill fluxes.

The effective Zn transport rates, i.e., the fluxes J, in the MHS were then evaluated from the experimental data given in Fig. 3. Before calculating the fluxes, the concentration data were recalculated to the cumulative amount of Zn(II) (Q) in the strip phase vs time. The slope of a tangent drawn to a respective Q vs time curve in its linear region indicates the effective mass transfer rate expressed in mol/cm^2·s:

$$Q = V_s[Zn]_s/1000A_s = J \times t + \text{constant} \qquad (9)$$

The symbols in Eq. (6) denote Q in mol/cm^2 is the total amount of Zn transferred from the membrane phase to the strip solution through 1 cm^2 of the strip IEM, V_s is the volume of the strip solution (cm^3), A_s is the strip membrane area, and $[Zn]_s$ is the time-dependent concentration of zinc in the strip solution (mol/dm^3). The same flux can be calculated for the feed solution and interface, i.e., from $[Zn]_f$ vs t dependence when $J_f = J_s$.

It is seen from Fig. 3 that experimental points, after a transient state, satisfy the condition of linearity predicted by Eq. (9). Within the standard confidence limits they fulfill a linearity with correlation coefficients above 0.95. Table 2 lists all the results for the MHS studied together with fluxes corresponding with Fig. 3. These values prove that preequilibration procedure results in a flux equal to $17.1 \pm 0.1 \times 10^{-11}$ whereas that evaluated for the "nonpreequilibrated system" is $3.9 \pm 0.3 \times 10^{-11}$ mol/cm^2·s, i.e., it remains far from its steady-state value. After lowering the concentration of D2EHPA in the liquid membrane from 0.1 to 0.01 mol/dm^3 (Curves 2 and 3 in Fig. 3), the results remain reasonable, i.e., the uphill flux is $10.8 \pm 0.6 \times 10^{-11}$ mol/m^2·s. Other characteristics associated with the MHS fluxes are the recovery factor (RF), and the concentration (enrichment) factor (CF) defined as follows:

$$RF = 100 \times (1 - [Zn]_{f,t}/[Zn]_{f,t=0}) \tag{10}$$

$$CF = [Zn]_{s,t}/[Zn]_{f,t=0} \tag{11}$$

For the considered transport Runs 2 and 3, the RF values after 30–35 hours of the MHS operation are 33–31% and the CF values range within 1.9–1.8. Also, for other transport runs the fluxes are constant in time for RF $<$ 30% and CF $<$ 2. The low influence of the feed depletion and the strip enrichment on the MHS operation is probably the result of the stabilizing function of the CEMs sorbing specifically zinc or hydrogen ions from their respective external solutions.

To compare our results with these presented by other authors (20, 28) we calculated additionally the effective permeability coefficients by using simple Eq. (12):

$$P = 1000 \times J/[Zn]_{f,0} \qquad \text{(cm/s)} \tag{12}$$

The values of P for each studied MHS are presented in Table 2. It should be explained, however, that the calculation of P originating from the diffusion–solution model of a membrane transport is a serious simplification in the case of coupled transport because the flux is dependent on both $[Zn]_{f,0}$ and $[H_2SO_4]_{s,0}$.

TABLE 2
Stationary Uphill Transport Fluxes of Zn(II) in Multimembrane Hybrid Systems of Various Composition and Operating Conditions

Run	Ion-exchange polymer membrane	Liquid membrane: [D2EHPA] (mol/dm^3)	Liquid membrane: Solvent	Feed-to-strip area ratio $A_f A_s$	Zero-time concentration of hydrogen ions in feed	Flux, $J \times 10^{11}$ (mol/cm^2·s), and effective permeability coefficient, $P \times 10^5$ (cm/s)
1	Nafion-120[a]	0.1	Kerosene	1:1	10^{-5}–10^{-4}	3.8 ± 0.3
2	Nafion-120	0.1	Kerosene	1:1	10^{-5}–10^{-4}	17.1 ± 0.1
3	Nafion-120	0.01	Kerosene	1:1	10^{-5}–10^{-4}	11.0 ± 1.0
4	Flemion	0.01	Kerosene	1:1	10^{-5}–10^{-4}	<1
5	Neosepta AFN-7	0.01	Kerosene	1:1	10^{-5}–10^{-4}	No flux
6	Nafion-117	0.01	Kerosene	1:1	10^{-5}–10^{-4}	5.8 ± 0.8
7	Raipore 4010	0.01	Kerosene	1:1	10^{-5}–10^{-4}	9.8 ± 0.3
8	MRF-26	0.01	Kerosene	1:1	10^{-5}–10^{-4}	4.2 ± 0.1
9	Neosepta CM-1	0.01	Kerosene	1:1	10^{-5}–10^{-4}	7.5 ± 0.9
10	Neosepta CM-2	0.01	Kerosene	1:1	10^{-5}–10^{-4}	9.1 ± 0.9
11	SPS-1	0.01	Kerosene	1:1	10^{-5}–10^{-4}	8.1 ± 0.4
12	SPS-2	0.01	Kerosene	1:1	10^{-5}–10^{-4}	12.3 ± 0.6
13	Nafion-117	0.01	*n*-Hexane	1:1	10^{-5}–10^{-4}	26.0 ± 1.0
14	Nafion-117	0.01	CCl_4	1:1	10^{-5}–10^{-4}	4.7 ± 0.3
15	Nafion-117	0.01	Toluene	1:1	10^{-5}–10^{-4}	23.1 ± 0.4
16	SPS-2	0.01	*n*-Hexane	1:1	10^{-5}–10^{-4}	13.0 ± 1.0
17	SPS-2	0.01	CCl_4	1:1	10^{-5}–10^{-4}	4.6 ± 0.2
18	Nafion-117	0.01	Kerosene	3:1	10^{-5}–10^{-4}	17.3 ± 0.5
19	Nafion-117	0.01	Kerosene	1:3	10^{-5}–10^{-4}	6.1 ± 0.5
20	SPS-2	0.01	Kerosene	3:1	10^{-5}–10^{-4}	13.5 ± 0.5
21	SPS-2	0.01	Kerosene	1:3	10^{-5}–10^{-4}	5.7 ± 0.1
22	Nafion-117	0.01	Kerosene	1:1	0.001	6.7 ± 0.2
23	Nafion-117	0.01	Kerosene	1:1	0.01	1.6 ± 0.01
24	SPS-2	0.01	Kerosene	1:1	0.001	3.8 ± 0.3
25	SPS-2	0.01	Kerosene	1:1	0.01	1.9 ± 0.1

[a] The membrane was initially in its hydrogen form.

MARCEL DEKKER, INC.
270 Madison Avenue, New York, New York 10016

Effect of IEM Functional Groups

In order to support the proposed transport mechanism (see Fig. 1) with ion-exchange reactions mediating the feed and strip processes, the external cation-exchange membranes of different functional groups were used. The MHS performances with sulfonic acid (Nafion-120), carboxylic acid (Flemion), and amine (Neosepta AFN-7) groups are illustrated by using the Q vs t plots in Fig. 4. The comparison of Zn(II) cumulative curves in Fig. 4 shows that little transport of Zn(II) occurs when the carboxylic membranes are used as intermediating layers between the LM and an acidic receiving solution. The flux is small when compared with other fluxes in Table 2, and reaches $\sim 1 \times 10^{-11}$ mol/cm^2·s. As expected from the transport mechanism in Fig. 1, the effective flux was observed only for the CEMs with sulfonic acid functional groups. The use of a hydrophilic membrane with anion-exchanging sites does not allow the transport to be reached. Thus, any other diffusion process in the IEMs, except for an efficient throughout ion-exchange diffusion, does not result in MHS transport. One can note, however, that as reported by Kislik and Eyal (17), it is possible to transport metal species in the MHS with anion-exchange membranes (AEMs) after forming neutral molecules (or ion pairs) in the feed phase. In this case the AEMs play the role of a hydrophilic porous interface material (contactor). Another possibility is the diffusion of free electrolyte

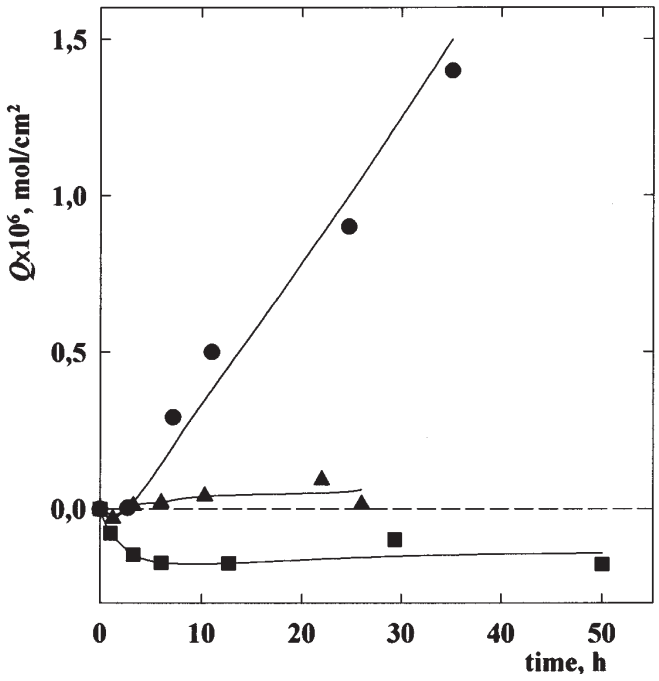

FIG. 4 Comparison of cumulative curves for uphill transport runs in the MHS with (●) Nafion-120, (■) Neosepta AFN-7, and (▲) Flemion membranes.

MARCEL DEKKER, INC.
270 Madison Avenue, New York, New York 10016

through the AEM (18). This process, however, seems to be negligible in the MHS.

Effect of CEM Characteristics

The objective of this investigation was to optimize the MHS properties by a proper selection of the ion-exchange polymer membranes. The membranes, made of different polymeric backbones but always with sulfonic ion-exchange sites, were taken into consideration. Some of them, i.e., perfluorinated polymer (Nafion), polystyrene (Neosepta CM-1 and 2), and polysulfone (SPS-1,2)-based membranes, differ greatly in their structures. The Nafion membranes are of clustered morphology (19), the Neosepta membranes contain gel-type crosslinked polyelectrolyte, and the SPS-1 and 2 are typical asymmetric porous/microporous membranes (14). The results presented in Fig. 5(A–C) and the fluxes summarized in Table 2 can be analyzed after taking into account the density of fixed charges inside the CEM and the membrane thickness (see Table 1).

From the results presented one can expect that fluxes in the MHS can be proportional to the density of fixed charged groups in the CEM used and inversely proportional to its thickness on the condition that the carrier concentration in the BLM does not limit the overall transport process. To check this hypothesis, we tried to correlate the fluxes from Table 2 with the ratio of fixed

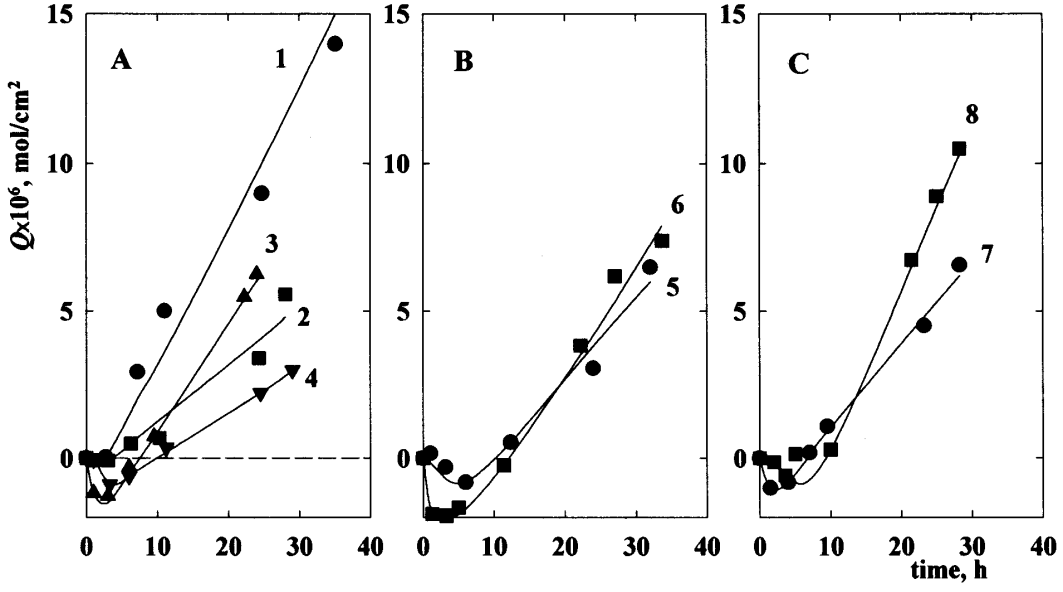

FIG. 5 Transport curves for MHS with sulfonic membranes made of different polymers. (A) Perfluorinated or fluorinate polymer: Nafion-120 (1), Nafion-117 (2), Raipore 4010 (3), MRF-26 (4). (B) Polystyrene-based membranes: Neosepta CM-1 (5), CM-2 (6). (C) Polysulfone: SPS-1 (7), SPS-2 (8).

MARCEL DEKKER, INC.
270 Madison Avenue, New York, New York 10016

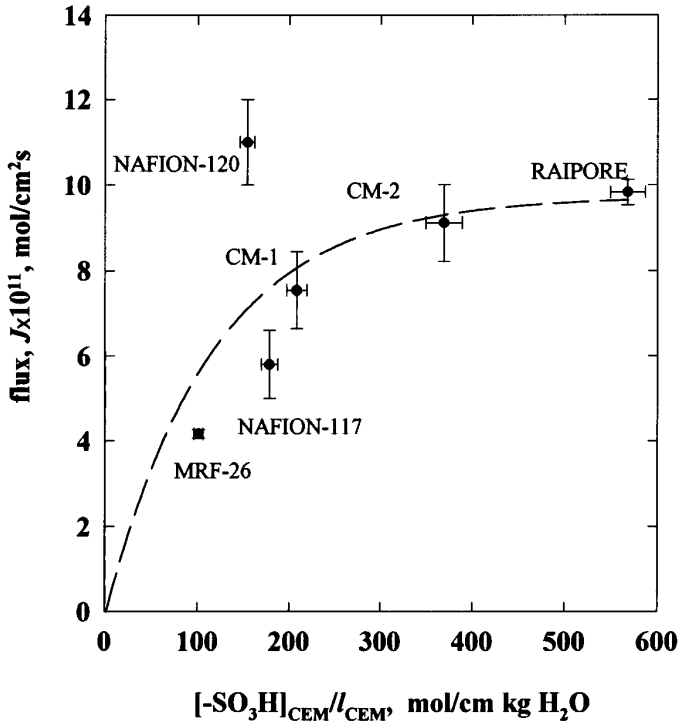

FIG. 6 Dependence of fluxes on the ratio of fixed charge density and the thickness of cation-exchange membranes.

sites concentration [—SO_3H] to the membrane thickness l_{CEM}. The respective plot for the MHSs containing a BLM of the same composition (0.01 M D2EHPA in kerosene) is presented in Fig. 6. The curve exhibits the saturation tendency, indicating trivially that thin and highly charged CEMs, independent of their composition and structure (e.g., Nafion, CM, Raipore, MRF), do not limit the MHS transport. Some scattering of the data for Nafion-120 and other membranes can be ascribed to some differences in their water content and possible differences in tortuosity of diffusion pathways. The properties of MHS with SPS membranes cannot be interpreted directly in the same way because their structure is completely different. However, the fluxes equal to 8.1×10^{-11} (SPS-1) and 12.3×10^{-11} (SPS-2) mol/cm^2·s, seem to be characteristic for membranes with a [—SO_3H]/l_{CEM} ratio higher than 300.

In general, there are no drastic differences among the MHS systems with quite different CEMs containing sulfonic acid groups. This result is consistent with the transport properties of some other MHSs reported previously by Kedem et al. (20, 28). Unexpectedly, there are no special differences between perfluorosulfonic and polystyrenesulfonic acid membranes. These differences could be expected because the perfluorinated backbone lowers electrostatic interactions between ion-exchange sites and counterions (21). Thus, in com-

parison to other membranes, the lower sorption selectivity of Zn(II) cation should enable higher interdiffusion fluxes for Zn(II)/H.

As expected, the results obtained with the laboratory-made SPS membranes are quite satisfactory or better than these obtained with commercially available membranes due to their specific structures. After considering these results, the Nafion-117 (currently commercially available) and the SPS-2 membranes were selected for further studies.

Effect of Liquid Membrane (LM) Solvent

In order to evaluate MHS transport as dependent on the composition of the liquid membrane, different solvents were used to prepare the LM, i.e., kerosene, carbon tetrachloride, hexane, and toluene with the same amount of the dissolved D2EHPA (0.01 mol/dm^3). Two experimental series, i.e., one with the Nafion-117 and another with the SPS-2 membranes, were carried out. Experimental data illustrating significant differences in Zn(II) transport are presented in Fig. 7(A, B). The plots in Fig. 7(B) show that transport rates are dependent on the viscosity of the liquid membrane phase. It can be concluded that the influence of a solvent on the MHS ability to transport Zn(II) is more important than the influence of the CEM composition. Thus, the system additionally exhibits the properties characteristic for a liquid membrane system, which implies that the solvent or BLM viscosity should be considered as one of the main parameters for optimizing the MHS properties. Certainly, there are some limitations due to possible deterioration of the CEM backbone and structure. For example, toluene cannot be used for the MHS with the polysulfone-based membranes. On the other hand, the membranes made of perfluorinated polymers are resistant to most of solvents used in liquid membrane technology. It was checked by other experiments that these membranes did not change their transport properties after more than 2000 hours of operation in a MHS (29). Some deformation of their surface and increased swelling were observed only after a long-time contact with the BLM containing 1,2-dichloroethane. We also showed that the membranes based on polystyrene sulfonic acid remain unchanged after using them in a MHS operating continuously for 800 hours (30). Nevertheless, depending on the CEM and the BLM composition, some unknown effects resulting from the sorption of organic solvent into hydrophobic components of CEM are possible (e.g., PVC in Tokuyama Soda CM membranes).

From the theoretical point of view there is, however, another more interesting and unrecognized problem concerning the structure and composition of the CEM/BLM interface. Unfortunately, the physicochemical properties of CEMs contacted with hydrophobic liquid exchangers, such as the solution of D2EHPA in kerosene or other solvents, are not recognized. We hope that these properties will be studied more intensively when MHS gains practical importance.

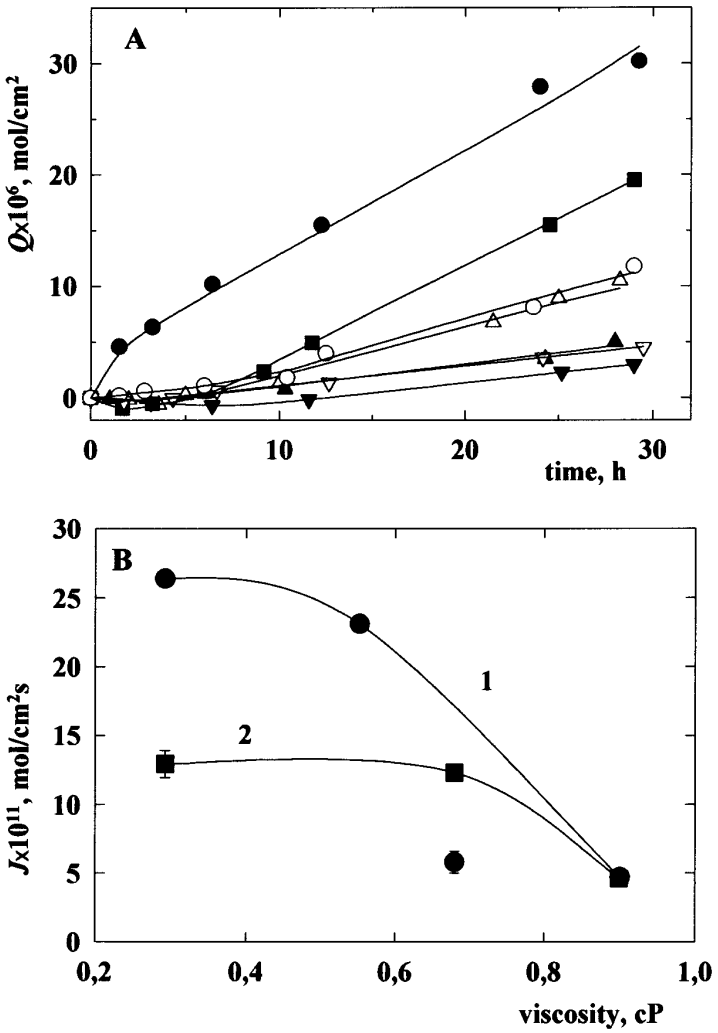

FIG. 7 The effect of liquid membrane solvent on MHS performances. (A) (○, ●) n-Hexane, (△, ▲) kerosene, (▽, ▼) carbon tetrachloride, and (■) toluene with Nafion-117 (filled symbols) or SPS-2 (empty symbols). (B) Effect of solvent viscosity on fluxes: Nafion-117 (1), SPS-2 (2)

Effect of System Configuration

The mass transfer data found in liquid membrane systems are not always reliable because of the changeable area of the respective aqueous/organic phase interfaces. The MHS and the cell used in this study enabled us to evaluate the influence of the feed and strip area on the uphill fluxes. The experimental curves for Nafion-117 and SPS-2 membranes contacted with the kerosene/D2EHPA liquid membrane are presented in Fig. 8(A, B). The curves correspond to MHSs with feed-to-strip interface area ratios equal to 3:1, 1:1,

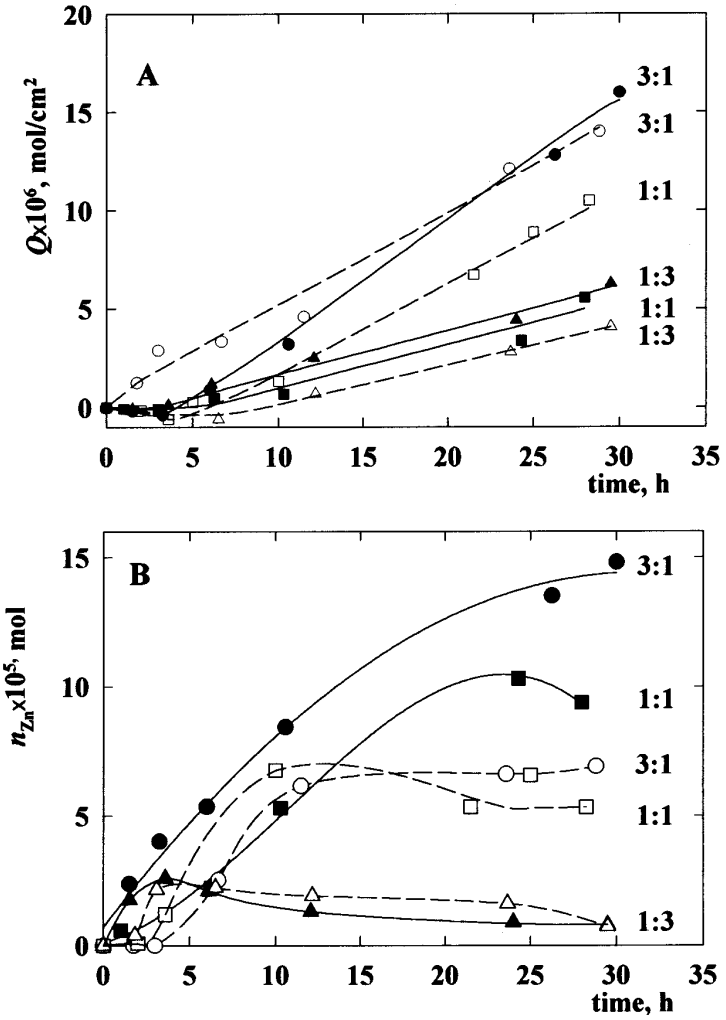

FIG. 8 Transport and Zn(II) accumulation in MHS on system asymmetry. The Af/As ratio is given at the respective curve. MHS with Nafion-117 (——, filled symbols) or SPS-2 (- - -, empty symbols) membrane. (A) Transport curves, (B) accumulation vs time.

and 1:3. It should be noted that the transport processes mediated by ion-exchange groups in CEMs and by the carrier in a liquid membrane can differ in their rates. Moreover, the ion-exchange reactions are reversible, and their forward and back counterparts can also occur with different rates. Thus, a fast feed process may mean a slower strip process and vice versa. This nonequivalence usually causes some accumulation of transported species in a liquid membrane phase. This accumulation is not important in technological processes but it should be taken into account in some analytical preconcentrations where the retention of analyzed species outside the strip solution should be as low as possible (31). The accumulation (n_{Zn} in moles) was calculated from the

mass balance of zinc in the feed and strip solutions, i.e., from the difference between the initial content of zinc in aqueous solutions and the content after time *t*:

$$n_{Zn} = (V_f[Zn]_{f,0} + V_{s,0}[Zn]_{s,0}) - (V_f[Zn]_{f,t} + V_s[Zn]_{s,t}) \quad (13)$$

Thus, n_{Zn} denotes the number of Zn moles accumulated from the external solutions by the MHS components. Because the CEMs were preequilibrated with these solutions, one can expect that n_{Zn} denotes mainly the accumulation of Zn(II) in the BLM by D2EHPA. The results presented in Fig. 8(B) show that the overall amount of Zn(II) accumulated in the MHS is the lowest when the stripping area (A_s) is higher than that of the feed area (A_f). The concentration of zinc in the BLM, $[Zn]_{BLM}$, can be evaluated by dividing n_{Zn} by V_{BLM} (35 cm^3) under the assumption that the composition of the preequilibrated CEMs does not change significantly over time. For the data presented in Fig 8, the lower and upper limits for $[Zn]_{BLM}$ are 2.9×10^{-4} and 4.3×10^{-3} mol/dm^3, respectively. This also means that the systems operated at a carrier loading, $2[Zn]_{BLM}/[D2EHPA]_{BLM}$, ranging from 0.058 to 0.86.

The fluxes are also dependent on the A_f/A_s ratio, and they increase with an increase in this ratio. This effect is caused by a higher concentration of the D2EHPA(Zn) complex in the BLM phase as well as by more favorable conditions for the stripping reaction leading to high output fluxes of Zn(II).

Effect of Concentration of H^+ Ions in Feed

The pH of feeds (pH_f) taken from industrial wastewaters may vary over a wide range. On the other hand, the properties of D2EHPA acting as the Zn(II) carrier are strongly dependent on pH_f (22), i.e., a low pH_f makes this reagent ineffective as an extractant of Zn(II) (23). To evaluate the dependence of the uphill transport fluxes on the concentration of hydrogen ions in the feed, some additional transport runs were carried out by using feeds with added sulfuric acid. The ability of the MHS to concentrate Zn(II) at various starting $[H]_{f,0}$ values was tested for the Nafion and SPS-2 membranes. The correlation between this concentration and the Zn(II) fluxes is presented in Fig. 9. The respective plots indicate that an increased concentration of hydrogen ions in the feed causes a decrease in the fluxes. However, depending on the membrane structure, this effect can be different, i.e., in the $\log[H]_{f,0}$ range 5–2 the flux of Zn(II) decreases 3-fold in the case of the Nafion-117 membrane and 6-fold in the case of the SPS-2 membrane. This might account for a lower average concentration of fixed groups in the SPS-2 membrane and, thus, its lower ability to exclude free sulfuric acid according to the Donnan equilibrium rule. The highly porous structure of the SPS-2 membrane makes its resistivity to the influx of the acidic feed into the membrane phase lower as compared with the

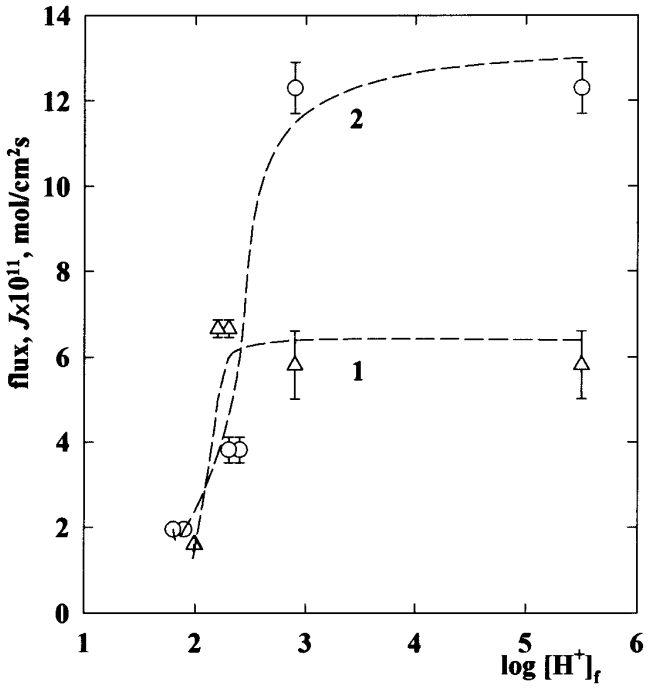

FIG. 9 Dependence of fluxes on the concentration of hydrogen ions in the feed: MHS with Nafion-117 (1) or SPS-2 (2) membranes.

dense Nafion membrane. Thus, despite quite high fluxes, the SPS membrane, when compared with membranes of a gelatinous structure, can operate efficiently in a system with a lower concentration of H^+ in the feed. In respect to dense ion-exchange membranes with a high fixed charge density, it should be noted that free acid cannot be sorbed from dilute solutions into the membrane phase because of their permselectivity. Thus, other factors influencing the fluxes after acidification of the feed should be taken into account. Without ranking their contribution, one can itemize such phenomena as competitive ion-exchange sorption of H^+ into the CEM phase (when the concentration of H_2SO_4 in the feed is comparable or exceeds the concentration of $ZnSO_4$) (i), diminished difference of H^+ concentrations (ii), and diminished concentration of Zn(II) after their association with anions in the feed (iii).

CONCLUSIONS

It was anticipated and is herein demonstrated that MHSs can operate efficiently only when ion-exchange reactions between solutions and charged polymer membranes are allowed. The fluxes are dependent on the characteristics of both the CEM and BLM used for the MHS construction. The basic pa-

MARCEL DEKKER, INC.
270 Madison Avenue, New York, New York 10016

rameters for optimizing MHS performance are the density of fixed charged groups in CEM (i), the CEM thickness (ii), and the viscosity of D2EHPA solvent used for the BLM preparation (iii). The coupling of cation-exchange processes inside the CEMs to the reaction–diffusion processes involving carrier molecules in the BLM is fundamental for MHS operation. The effective permeability coefficients (P) of Zn(II) for MHSs containing D2EHPA and various strong acid CEMs are in the range 4×10^{-5} to 1.2×10^{-4} mol/cm (see Table 2). These results are comparable with the results published by Kedem et al. (20, 28) for Cu(II) (2.7×10^{-5} cm/s) and Ag^{+} (8.6×10^{-5} cm/s) transports performed in MHSs containing LIX64 and di(2-ethylhexyl)thiophosphoric acid, respectively.

The use of the strong acid CEMs as intermediating layers in a MHS provides an efficient uphill transport of Zn(II). Among commercially available membranes, the perfluorinated sulfonic acid membrane Nafion-117 seems the most preferable, although there are no obstacles to use some other membranes containing a large amount of polyanionic component. The Nafion membranes collaborate well with hydrophobic liquid membranes made of various organic solvents because of their good mechanical properties and small water leakage. Laboratory-made porous sulfonated polysulfone membranes provide similar results, but their use should be limited to a higher pH of the feed phase. In respect to the BLM composition, a membrane made of hexane is the most efficient due to its low viscosity when compared to kerosene, toluene, and carbon tetrachloride. The input and output fluxes in a MHS, the nonequivalence of which leads to the accumulation of transported species in the MHS components, can be diminished by augmenting the strip interface area. If accumulation can be neglected, the fluxes can be substantially augmented by increasing the ratio of the feed-to-strip area interfaces.

ACKNOWLEDGMENT

This research was financially supported through a grant from Nicolous Copernicus University, Project CH-373.

REFERENCES

1. R. Wódzki and G. Sionkowski, *Sep. Sci. Technol., 30,* 2763 (1995).
2. R. Wódzki and G. Sionkowski, *Ibid., 31,* 1541 (1995).
3. R. Wódzki and J. Nowaczyk, *Solv. Extr. Ion Exch., 15,* 1085 (1997).
4. R. Marr, A. Bouvier, J. Draxler, M. Prötsch, and A. Kriechbaumer, *Proc. PACHEC'98, Seoul, Korea, Vol. I,* 1983 pp. 327–332.
5. G. Sionkowski and R. Wódzki, *Sep. Sci. Technol., 30,* 805 (1995).
6. J. P. Behr, M. Kirch, and J. M. Lehn, *J. Am. Chem. Soc., 107,* 241 (1985).
7. R. Wódzki, *Pol. J. Chem., 63,* 557 (1989).
8. R. Wódzki, *Ibid., 65,* 1715 (1991).

MARCEL DEKKER, INC.
270 Madison Avenue, New York, New York 10016

9. N. Lakshminarayanaiah, *Transport Phenomena in Membranes*, Academic Press, New York, NY, 1969, pp. 158–175.
10. E. L. Cussler, R. Aris, and A. Bhown, *J. Membr. Sci.*, *43*, 149 (1989).
11. C. P. Wen and H. F. Hamil, *Ibid*., *8*, 51 (1981).
12. G. Oster, A. Perelson, and A. Katchalsky, *Q. Rev. Biophys*., *6*, 1 (1973).
13. R. Wódzki and G. Sionkowski, *Pol. J. Chem*., *69*, 407 (1995).
14. M. Kabsch-Korbutowicz, G. Poźniak, W. Trochimczuk, and T. Winnicki, *Sep. Sci. Technol*., *29*, 2345 (1994).
15. C. Brousse, R. Chapurlat, and J. P. Quentin, *Desalination*, *18*, 137 (1976).
16. N. Shivashinsky and G. B. Tanny, *J. Appl. Polym. Sci*., *28*, 3235 (1983).
17. V. S. Kislik and A. M. Eyal, *J. Membr. Sci*., *111*, 273 (1996).
18. A. Narębska and A. Warszawski, *Sep. Sci. Technol*., *27*, 703 (1992).
19. K. A. Mauritz and A. J. Hopfinger, "Structural Properties of Membrane Ionomers," in *Modern Aspects of Electrochemistry, No. 14* (J. O. M. Bockris, B. E. Conway, and R. E. White, Eds.), Plenum Publishing, NY, 1982.
20. O. Kedem, L. Bromberg, and A. M. Eyal, *European Patent Application* EP 0 574 717 A2 (1993).
21. A. Steck and H. L. Yeager, *Anal. Chem*., *52*, 1215 (1980).
22. L. Fernandez, J. Aparicio, and M. Muhammed, *Sep. Sci. Technol*., *22*, 1577 (1987).
23. M. Kunzmann and Z. Kolarik, *Solv. Extr. Ion Exch*., *10*, 35 (1992).
24. D. J. Vaughan, *Du Pont Innovation*, *4*, 10 (1973).
25. Yu. Vautskij, M. G. Rhyzov, and A. M. Lalin, *Plast. Massy*, p. 39 (1976).
26. M. Suhara, K. Suzuki, H. Horie, and T. Shimoira, *J. Membr. Sci*., *41*, 143 (1989).
27. *Neosepta Ion Exchange Membranes*, Information Booklet, Tokuyama Soda Co., Ltd.
28. O. Kedem and L. Bromberg, *J. Membr. Sci*., *78*, 255 (1993).
29. R. Wódzki, M. Świątkowski, and G. Łapienis, submitted for publication in *Macromol. Chem. Phys*.
30. R. Wódzki and P. Szczepański, *Mat. Int. Conf.* "*Forum Chemiczne*", Warsaw, 1998, Abstract P53.
31. P. Rajec, V. Mikulaj, and J. Macková, *J. Radioanal. Nucl. Chem., Articles*, *150*, 315 (1991).

Received by editor October 29, 1997
Revision received June 1998

PAGE 650 IS BLANK

MARCEL DEKKER, INC.
270 Madison Avenue, New York, New York 10016

Request Permission or Order Reprints Instantly!